Int. J. Solids Structures, 1971, Vol. 7, pp. 83 to 97. Pergamon Press. Printed in Great Britain

NUMERICAL SOLUTION OF NON-LINEAR CREEP PROBLEMS WITH APPLICATION TO PLATES

Z. P. BAŽANT†

The Technological Institute, Northwestern University, Evanston, Illinois

Abstract—A general numerical method of time integration of non-linear integral-type creep problems is presented. This method reduces the creep problem to a sequence of elasticity problems with initial strains. Its practical feasibility and convergence is proved by the analysis of a rectangular plate, and the accuracy of various types of the method is empirically studied. For the special case of a degenerate memory function, an efficient, storage and time saving modification is derived. In addition, the numerical methods for rate-type creep are also studied.

1. INTRODUCTION

IT IS well-known that an inelastic stress problem can be approximately solved as a sequence of linear elastic problems. This method is based on Theorem I given in the Appendix. This theorem allows to convert the elasticity problem with initial strains to an elasticity problem without initial strains. For volumetric strains this theorem was presented in 1838 by Duhamel, for deviatoric strains and isotropic material it was derived in 1931 by Reissner (see [1]). By different approaches it was later independently obtained by Eschelby (cf. [1]) and (for a generally anisotropic material) by Bažant [2–4]. First application of this theorem to creep (of the rate type) of plates is due to Lin [5, 1] and Bažant [3, 4]. In these studies only simple examples, accessible to hand calculation and serving merely the purpose of illustration, were solved numerically [5, 1]; in space coordinates the finite difference method was considered. Without recourse to Theorem 1, a conversion of initial strains to nodal loads, equivalent to this theorem, has been developed for the finite element method (cf. [6]).

In this paper‡ a method of solution of non-linear integral-type problems based on Theorem I will be shown and applied to plate bending. The solution for the rate-type creep will be also discussed. Practical feasibility and convergence of solution will be proved by the results of computer analysis and the rate of convergence will be studied by means of examples.

2. ALGORITHM OF TIME INTEGRATION FOR INTEGRAL-TYPE CREEP

Let the following isotropic non-linear creep law for small deformations be considered:

$$\left.\begin{aligned} \varepsilon_v(t) &= \frac{\sigma_v(t)}{K} + \int_{t_0}^{t} \frac{\sigma_v(\tau)}{K} F_v(\tau) L_v(t,\tau)\,\mathrm{d}\tau \\ e_{ij}(t) &= \frac{s_{ij}(t)}{2G} + \int_{t_0}^{t} \frac{s_{ij}(\tau)}{2G} F_d(\tau) L_d(t,\tau)\,\mathrm{d}\tau \qquad (i,j = 1,2,3) \end{aligned}\right\} \tag{1}$$

† Associate Professor of Civil Engineering.

‡ This paper is based on author's Internal Research Report No. 68/2, "Approximate Analysis of Linear and Nonlinear Creep Problems. Initial Strain Method", Department of Civil Engineering, University of Toronto (1968).

where t = time, t_0 = time of first loading, τ = time as integration variable; σ_v, ε_v = volumetric stress and strain; s_{ij}, e_{ij} = deviators of stress and strain in cartesian coordinates $x = x_1$, $y = x_2$, $z = x_3$; L_v, L_d = given memory functions; K = volumetric modulus, G = shear modulus; F_v, F_d = given polynomials in the basic invariants of the stress tensor in time τ. In the numerical example it will be assumed:

$$F_v(\tau) = 1 + [\sigma_v(\tau)/400]^2, \qquad F_d(\tau) = 1 + [\bar{s}(\tau)/250]^2 \tag{2}$$

where σ_v and $\bar{s}$ are expressed in kp (force kilogram)/cm^2; $\bar{s}$ = stress intensity. For plane stress ($\sigma_{33} = \sigma_{13} = \sigma_{23} = 0$),

$$\bar{s}^2 = (\sigma_{11} - \sigma_{22})^2 + \sigma_{11}\sigma_{22} + 3\sigma_{12}^2 \tag{3}$$

where $\sigma_{ij} = s_{ij} + \delta_{ij}\sigma_v$ = stress tensor, δ_{ij} = Kronecker delta. The memory functions will be assumed in the numerical example as follows

$$\left.\begin{aligned} L_d(t,\tau) &= -\frac{\partial}{\partial\tau}\left[\left(0{\cdot}6 + \frac{100}{\tau}\right)\frac{t-\tau}{t-\tau+60}\right] \\ L_v(t,\tau) &= L_d(t,\tau)(0{\cdot}5-\mu')/(1+\mu') \end{aligned}\right\}. \tag{4}$$

where μ' = Poisson ratio for creep. These memory functions may be used for cement concrete at constant humidity and temperature; t and τ represent the age of concrete and in (4) are assumed to be given in days.

Introducing a subdivision $t_{(0)}, t_{(1)}, \ldots t_{(n)}$ of the given time interval (t_0, t_1) into n equal subintervals Δt, the hereditary integrals in equation (1) for $t = t_{(r)}$ may be approximated by the following expressions

$$\varepsilon^0_{v(r)} = \sigma^0_{v(r)}/K, \qquad e^0_{ij(r)} = s^0_{ij(r)}/2G \tag{5}$$

where

$$\left.\begin{aligned} \sigma^0_{v(r)} &= \sum_{s=0}^{r} c'_{(s)}\sigma_{v(s)}F_{v(s)}L_v(t_{(r)}, t_{(s)}) \\ s^0_{ij(r)} &= \sum_{s=0}^{r} c'_{(s)}s_{ij(s)}F_{d(s)}L_d(t_{(r)}, t_{(s)}) \qquad (i,j = 1,2,3) \end{aligned}\right\}. \tag{6}$$

Subscript (r) stands for time $t_{(r)}$, e.g. $\sigma_{v(s)} = \sigma_v(t_{(s)})$; $c'_{(s)}$ = coefficients of the formula for numerical integration. The creep law (1) may now be written in the form

$$\varepsilon_{v(r)} = \sigma_{v(r)}/K + \varepsilon^0_{v(r)}, \qquad e_{ij(r)} = s_{ij(r)}/2G + e^0_{ij(r)} \qquad (i,j = 1,2,3). \tag{7}$$

If in a given creep problem the stresses have already been calculated up to the time $t_{(r-1)}$ and an estimate of the values in time $t_{(r)}$ has been made (by extrapolation), the values $e^0_{ij(r)}$ and $\varepsilon^0_{v(r)}$ may be determined, using equation (5). Equations (6) may then be regarded as a fictitious linear elastic stress–strain law with prescribed initial strains $\varepsilon^0_v, e^0_{ij}$. The calculation of $\sigma_{ij(r)}$ and $\varepsilon_{ij(r)}$ is therefore a problem of elasticity with initial strains. This problem may be converted to an elasticity problem without initial strains according to Theorem 1. The loads to be considered are the given applied loads (and the prescribed displacements) for time $t_{(r)}$. Solution of this elasticity problem yields the stresses, strains and displacements in time $t_{(r)}$. Calculating $e^0_{ij(r)}$ and $\varepsilon^0_{v(r)}$ again for these values of stress, and repeating the solution of the elasticity problem with initial strains, more accurate values of stresses, strains and displacements in time $t_{(r)}$ may be obtained.

Accuracy of the above algorithm depends essentially on the formula (5) for the evaluation of the hereditary integrals. The error is of order Δt^4 if the coefficients $c'_{(s)}$ are introduced according to the formula

$$\int_{t_{(0)}}^{t_{(r)}} f(t)\,dt \doteq \frac{\Delta t}{24}\Big[9(f_{(0)}+f_{(r)}) + 19(f_{(1)}+f_{(r-1)}) - 5(f_{(2)}+f_{(r-2)}) + f_{(3)} + f_{(r-3)} + \sum_{s=1}^{r-2}(-f_{(s-1)} + 13f_{(s)} + 13f_{(s+1)} - f_{(s-2)})\Big] \tag{8}$$

which is valid for $r \geq 3$ (both even and odd). For $r = 2$ the Simpson rule may be used. However, a special procedure is needed for $r = 1$ in order to maintain the same order of error and avoid the trapezoidal rule which would give an error of order Δt^2. This can be achieved by successive approximations over the first three steps Δt, as follows. First the approximate values of $\sigma_{ij(0)}, \sigma_{ij(1)}, \sigma_{ij(2)}$ and $\sigma_{ij(3)}$ are determined; most simply $\sigma_{ij(3)} = \sigma_{ij(2)} = \sigma_{ij(1)} = \sigma_{ij(0)}$ may be introduced. Then the values $\sigma_{ij(0.5)}$ for the middle of the first interval $(t_{(0)}, t_{(1)})$ are computed, using a 4th order interpolation formula which is $\sigma_{ij(0.5)} = (5\sigma_{ij(0)} + 15\sigma_{ij(1)} - 5\sigma_{ij(2)} + \sigma_{ij(3)})/16$. Subsequently the values $\sigma^0_{ij(1)}, \sigma^0_{ij(2)}, \sigma^0_{ij(3)}$ are computed, using solely the values $\sigma_{ij(r)}$ of the preceding approximation. The values $\sigma_{ij(0.5)}$ enable to apply the Simpson rule for the calculation of $\sigma_{ij(1)}$.

The algorithm of integration, just described, is represented by a flow chart in Fig. 1. **SUB1** $(\sigma_{ij}, w, \sigma^0_{ij})$ is a subroutine for the solution of the elasticity problem with initial stresses σ^0_{ij} as the input values; in the case of a plate this solution is carried out according

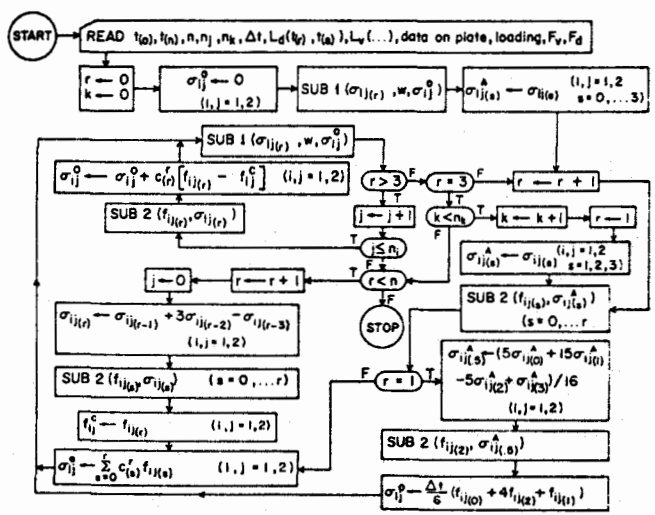

FIG. 1. Flow chart of the fourth-order method in the case of integral-type creep, valid for $n \geq 3$ (n = subdivision of time; n_j = number of iterations; n_k = number of approximations; T = true, F = false; SUB1, SUB2 = subroutines defined in the text).

to equations (A4), (A6)–(A10); SUB1 also includes the elastic solution of w and σ_{ij}, caused by the given applied loads in time $t_{(r)}$, and adds these values to the values due to initial stresses σ_{ij}^0. SUB2 (f_{ij}, σ_{ij}) is a subroutine which, using the values σ_{ij}, evaluates the integrands (denoted by f_{ij}) of the hereditary integrals in terms of the total stresses $\sigma_{ij}^0 = s_{ij}^0 + \delta_{ij}\sigma_v^0$ [rather than σ_v^0 and s_{ij}^0 as in equation (6)]; this is done according to equations (A1), (3), (2), (5) in this order, followed by

$$\tau_v \leftarrow \sigma_v F_v L_v(t_{(r)}, t_{(s)}), \qquad \tau_{ij} \leftarrow F_d L_d(t_{(r)}, t_{(s)}),$$

$$f_{ij} \leftarrow \tau_{ij} + \sigma_{ij}\tau_v;$$

$\sigma^A_{ij(r)}$ and f^C_{ij} are auxiliary arrays for storage of the values of σ_{ij} and f_{ij}, and enable to save computing time.

The refined, highly accurate method of integration, just described, requires that the functions (e.g. σ_{11}) which are to be integrated in time (or extrapolated) are sufficiently smooth, i.e. continuous and possessing continuous first three time derivatives. This condition is satisfied if the given loading (applied loads and prescribed displacements) evolves as a sufficiently smooth function of time.

If the loading or some of its first three derivatives is piece-wise discontinuous in time, the above integration algorithm would have to be started after each discontinuity as in the first three steps. Such a procedure would be, however, quite cumbersome, especially in the case of many discontinuities. Therefore only the most simple step-by-step procedure is then justified. The subintervals must be selected so that discontinuities occur only at the ends of individual subintervals. The time-integrals (9) may be calculated by the trapezoidal or rectangular rule and there is no reason for a special procedure in the first steps; for the first estimate of $\sigma_{ij(r)}$ no extrapolation from the previous subintervals is possible and only such assumptions as $\sigma_{ij(r)} \approx 0$ or $\sigma_{ij(r)} = \sigma_{ij(r-1)}$ make sense.† The effect of sudden load increments which represents an elasticity problem, must be computed separately.

To verify the above method of integration in time and study its convergence, the solution of a rectangular plate has been programmed. The edges $x = 0$ and $x = a$ were considered as fixed, and the edges y

finite difference method has been used; the plate was subdivided by a rectangular grid with the steps $\Delta x = a/10$ and $\Delta y = b/10$ along x and y, and $\Delta z = d/12$ across the thickness of plate. The functions w, M_x^0, M_y^0, M_{xy}^0 were represented by two-dimensional arrays of nodal values, and $\sigma_{11}, \sigma_{22}, \sigma_{12}$ by three-dimensional arrays. The integrals (A4) over the thickness of plate were evaluated by Simpson rule.

The following values were assumed for computations: $a = b = 400$ cm, $d = 12$ cm, $E = 4 \times 10^5$ kp/cm² (kp = kilopond = force kilogram), $\mu = 0{\cdot}15$, $\mu' = 0{\cdot}05$, $t_0 = 60$ days, $t_1 = 180$ days. A constant, uniformly distributed load $q = 0{\cdot}7$ kp/cm², applied in time t_0 was considered.

The results of computer analysis (IBM 7094) are given in Table 1 for different numbers n of the subdivisions of the time interval (t_0, t_1). The results are graphically represented in Figs. 2(a, b and c).

† For linear integral-type creep, this simplest version of integration in time was suggested (without numerical verification) by Bažant in 1966 [2].

TABLE 1. NUMERICAL RESULTS FOR INTEGRAL-TYPE CREEP OF A PLATE

No. of iterations per step n_j	No. of approximations in first 3 steps n_k	Subdivision n	$x = a/2$ $y = b/2$ w	$x = a/2$ $y = b/2$ $z = a/2$ σ_x	$x = a/2$ $y = b/2$ $z = d/2$ σ_y	$x = b/3$ $y = b/6$ $z = d/2$ τ_{xy}	$x = a/3$ $y = b/2$ w
2	6	4	1·175	117·3	90·13	−15·0	0·8830
		8	1·1644	111·7	90·12	−19·1	0·8753
		16	1·15969	110·500	89·1199	−18·9089	0·871416
4	8	4	1·179	117·9	91·71	−17·4	0·8868
		8	1·1643	111·6	90·10	−19·2	0·8752
		16	1·15969	110·494	89·1169	−18·9090	0·871408
6	10	4	1·178	117·1	91·68	−18·2	0·8864
		8	1·1643	111·6	90·11	−19·2	0·8752
		16	1·15969	110·494	89·1171	−18·9091	0·871408

3. SIMPLIFICATION FOR A DEGENERATE MEMORY FUNCTION

Often the memory functions may be assumed in the form of a degenerate kernel [8],

$$L_v(t, \tau) = \sum_{\alpha=1}^{n_\alpha} A_{v_\alpha}(\tau)B_{v_\alpha}(t), \qquad L_d(t, \tau) = \sum_{\alpha=1}^{n_\alpha} A_{d_\alpha}(\tau)B_{d_\alpha}(t) \tag{9}$$

in which the number of terms, n_α, is small; A_{v_α}, B_{v_α}, A_{d_α}, B_{d_α} are functions of one variable. For instance the function often used for concrete, namely

$$L_v(t, \tau) = -\frac{\partial}{\partial\tau}[\varphi_\alpha(\tau)(1 - e^{\gamma_\alpha(\tau - t)})] \tag{10}$$

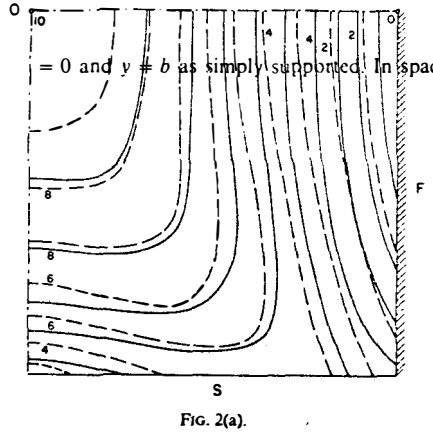

FIG. 2(a).

= 0 and $y \neq b$ as simply supported. In space coordinates the

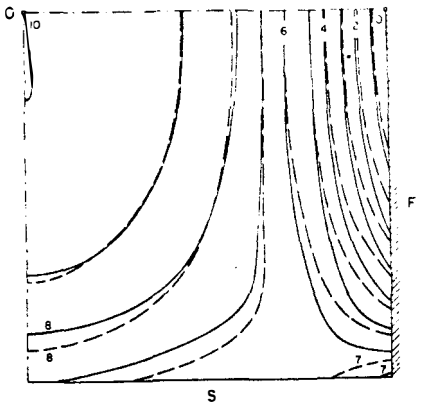

FIG. 2(b).

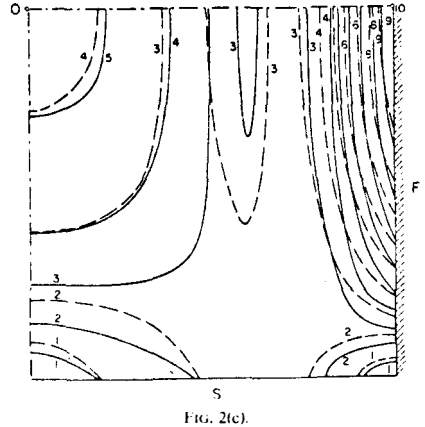

FIG. 2(c).

FIG. 2. Lines of equal relative values in the right lower quadrant of plate. Integral-type creep. (Dashed lines pertain to the initial state at the time t_0 of uniform load application, continuous lines to time t_1; S denotes the simple supported edge, F the fixed edge and 0 the center of plate.) (a) Maximum principal stresses at the lower face of plate; in time t_0, 0 corresponds to the stress value -48, 10 to 143·6; in time t_1, 0 corresponds to -84, 10 to 110·5. (b) Minimum principal stresses at the lower face; in time t_0, 0 corresponds to -315, 10 to 98·4; in time t_1, 0 corresponds to -218, 10 to 89·1. (c) Stress intensity at the faces; in time t_0, 0 corresponds to 0, 10 to 295; in time t_1, 0 corresponds to 0, 10 to 133.

in which φ_α are functions and γ_α constants, may be brought to the form (9). Substituting (9) into creep law (1), it follows

$$\sigma^0_{v_{(r)}} = \sum_\alpha B_{v_{\alpha(r)}} S_{v_{\alpha(r)}}, \qquad \sigma^0_{ij_{(r)}} = \sum_\alpha B_{d_{\alpha(r)}} S_{ij_{\alpha(r)}} \tag{11}$$

where

$$S_{v_{\alpha(r)}} = \int_0^{t_r} A_{v_\alpha}(\tau) F_v(\tau) \sigma_v(\tau)\, d\tau, \qquad S_{ij_{\alpha(r)}} = \int_0^{t_r} A_{d_\alpha}(\tau) F_d(\tau) s_{ij}(\tau)\, d\tau. \tag{12}$$

Replacing these integrals with a finite sum according to formula (8), the following recurrent relationships may be found (for $r > 3$):

$$S_{v_{\alpha(r)}} = S_{v_{\alpha(r-1)}} + \frac{\Delta t}{24}(8\varphi_{v_{(r)}} + 23\varphi_{v_{(r-1)}} - 11\varphi_{v_{(r-2)}} + 5\varphi_{v_{(r-3)}} - \varphi_{v_{(r-4)}}), \qquad S_{ij_{\alpha(r)}} = \ldots \tag{13}$$

where $\varphi_{v_{(r)}}$ denotes the value of $A_{v_{(r)}} F_{v_{(r)}} \sigma_{v_{(r)}}$. For $r = 3$,

$$S_{v_{\alpha(3)}} = \tfrac{3}{8}\Delta t(\varphi_{v_{(0)}} + 3\varphi_{v_{(1)}} + 3\varphi_{v_{(2)}} + \varphi_{v_{(3)}}). \tag{14}$$

In the case of a general memory function the need for storage of the entire history of stresses σ_{ij} in the computer memory may be a serious obstacle. Obviously, this may be circumvented if the memory functions are given in form (9) because it is sufficient to store only the history of stresses σ_{ij} over the last four steps, and the current values of $S_{11_\alpha} + S_{v_\alpha}$, $S_{22_\alpha} + S_{v_\alpha}$, S_{12_α} (in case of a plane problem) for all α, in addition. The amount of computer time for evaluation of σ^0_{ij} becomes also substantially reduced. The general form of the flow chart as it appears in Fig. 1 remains unchanged.

The recurrent relationship for S_{ij_α} and S_{v_α} is especially simple if the trapezoidal rule is used for the evaluation of integrals (12). Then

$$S_{v_{\alpha(r)}} = S_{v_{\alpha(r-1)}} + \frac{\Delta t}{2}(A_{v_{\alpha(r-1)}} F_{v_{\alpha(r-1)}} \sigma_{v_{\alpha(r-1)}} + A_{v_{\alpha(r)}} F_{v_{\alpha(r)}} \sigma_{v_{\alpha(r)}}), \qquad S_{ij_{\alpha(r)}} = \ldots \tag{15}$$

so that only the current values ($t = t_{(r)}$) and the last preceding values ($t = t_{(r-1)}$) of the stresses σ_{ij} need be stored. The starting values are $S_{v(0)} = S_{ij(0)} = 0$. The corresponding flow chart is given in Fig. 3.

It should be noted that in the case of a degenerate kernel [equation (9)] the non-linear integral-type creep law (1) may be converted to a rate-type creep law in form of a differential equation of order n_α.

4. ALGORITHM OF TIME INTEGRATION FOR RATE-TYPE CREEP

Consider now the following isotropic constitutive equation for small strains

$$\left.\begin{aligned} K(\dot\varepsilon_v + g_v \dot\varepsilon_v) &= \dot\sigma_v + f_v \sigma_v \\ 2G(\dot e_{ij} + g_d \dot e_{ij}) &= \dot s_{ij} + f_d s_{ij} \qquad (i, j = 1, 2, 3) \end{aligned}\right\} \tag{16}$$

where f_v, f_d, g_v, g_d = given polynomials in the invariants of the stress and strain tensors; $\dot\varepsilon_v$, $\dot e_{ij}$, $\dot\sigma_v$, $\dot s_{ij}$ = rates of strain and stress which may be taken (for small strains) as partial derivatives, e.g. $\dot\sigma_{ij} = \partial\sigma_{ij}/\partial t$. In the numerical example it has been assumed

$$f_v = g_v = g_d = 0, \qquad f_d = 0{\cdot}2 + \bar s^2/250^2. \tag{17}$$

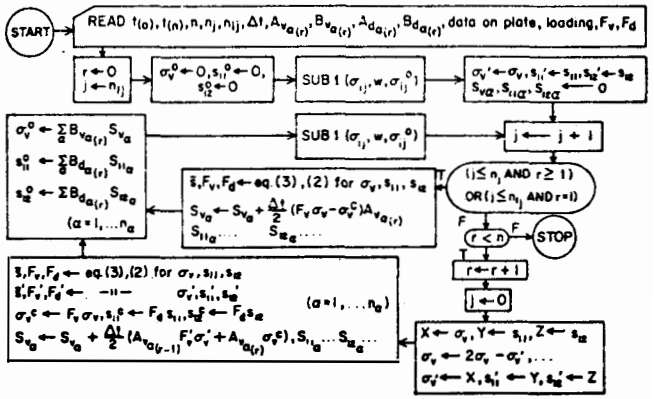

FIG. 3. Flow chart of the second-order method in the case of degenerate memory function for integral-type creep.

Subdiving the given time interval (t_0, t_1) as before, the creep law (16) may be approximated by the finite difference equations:

$$\Delta\varepsilon_{v_{(r)}} = \Delta\sigma_{v_{(r)}}/K + \varepsilon^0_{v_{(r)}}, \qquad \Delta e_{ij_{(r)}} = \Delta s_{ij_{(r)}}/2G + e^0_{ij_{(r)}} \qquad (i,j = 1,2,3) \tag{18}$$

where

$$\varepsilon^0_{v_{(r)}} = \sigma^0_{v_{(r)}}/K, \qquad e^0_{ij_{(r)}} = s^0_{ij_{(r)}}/2G \tag{19}$$

$$\left.\begin{aligned} \sigma^0_{v_{(r)}} &= (\bar{f}_v \bar{\sigma}_c - K\bar{g}_v \bar{\varepsilon}_c)\Delta t \\ e^0_{ij_{(r)}} &= (\bar{f}_d \bar{s}_{ij} - 2G\bar{g}_d \bar{e}_{ij})\Delta t \end{aligned}\right\} \tag{20}$$

Δ stands for increment from time $t_{(r-1)}$ to time $t_{(r)}$, e.g. $\Delta\varepsilon_{c_{(r)}} = \varepsilon_{c_{(r)}} - \varepsilon_{c_{(r-1)}}$; $\bar{f}_d, \bar{f}_v, \bar{s}_{ij}, \dots$ = certain values of $f_d, f_v, s_{ij}, \dots$ within the interval $[t_{(r-1)}, t_{(r)}]$.

Most simply the values of $\bar{f}_d, \bar{f}_v, \bar{s}_{ij}, \dots$ may be taken as the values of $f_d, f_v, s_{ij}, \dots$ in time $t_{(r-1)}$, i.e. $\bar{s}_{ij} = s_{ij_{(r-1)}}$ etc. the error in equation (18) being of order Δt. These values are available from the analysis of the preceding step $(t_{(r-2)}, t_{(r-1)})$ so that the values of $\varepsilon^0_{v_{(r)}}, e^0_{ij_{(r)}}$ in equation (18) may be determined. Thus equation (18) may be regarded as a fictitious incremental linear elastic stress-strain law with prescribed incremental initial strains $\varepsilon^0_c, e^0_{ij}$. The loads to be considered are the given applied load increments during the interval $[t_{(r-1)}, t_{(r)}]$. The calculation of $\Delta\sigma_{ij_{(r)}}$ and $\Delta\varepsilon_{ij_{(r)}}$ can be done again according to the Appendix.

A more accurate method whose error is proportional to Δt^2 may be arranged similarly as the second-order Runge–Kutta method for ordinary differential equations. Using the approximate values of $\Delta\sigma_{v_{(r)}}, \Delta s_{ij_{(r)}}, \Delta\varepsilon_{v_{(r)}}, \Delta e_{ij_{(r)}}$ obtained as above, $\varepsilon^0_{v_r}$, $e^0_{ij_{(r)}}$ (or $\sigma^0_{v_{(r)}}$, $s^0_{ij_{(r)}}$) may be recalculated from the following improved values

$$\bar{\sigma}_{ij} = \sigma_{ij_{(r-1)}} + \frac{1}{2}\Delta\sigma_{ij_{(r-1)}}, \quad \bar{\varepsilon}_{ij} = \varepsilon_{ij_{(r-1)}} + \frac{1}{2}\Delta\varepsilon_{ij_{(r-1)}} \tag{21}$$

with the corresponding $\bar{f}_v, \bar{f}_d, \bar{g}_v, \bar{g}_d$, and the analysis of $\Delta\sigma_{ij_{(r)}}, \Delta\varepsilon_{ij_{(r)}}$ repeated. The algorithm of this method is represented by the flow chart in Fig. 4. Subroutine SUB 1 is the same as in Fig. 1; SUB 3 $(\sigma^0_{ij}, \bar{\sigma}_{ij})$ is a subroutine which evaluates σ^0_{ij}, applying equations (A1), (3), (17), (20), (A5) in this order.

The second order method is, of course, justified only if the given loads and their first time derivative vary continuously with time within each time step. Contrary to the method in Fig. 1 for the integral-type creep, the loads and their derivatives may exhibit sudden increments (discontinuities) in times $t_{(r)}$ because no extrapolation from the previous interval is used. Determination of the effect of these sudden load increments is an elasticity problem.

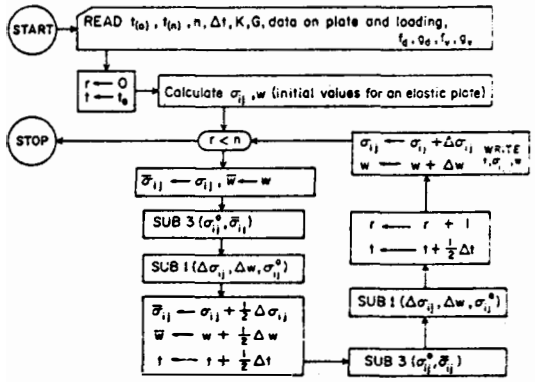

FIG. 4. Flow chart of the second-order method in the case of rate-type creep (n = subdivision of time, T = true, F = false).

The first order method is applicable for any piece-wise continuous time variation of loads, provided that the subintervals of time are selected so that discontinuities occur only at the ends of individual subintervals.

For verification, the same example as before has been programmed for the rate-type creep [equations (16), (17)]. The following numerical data were assumed:

$$a = b = 400\,\text{cm}, \; d = 12\,\text{cm}, \; E = 4\times10^5\,\text{kp cm}^{-2}, \; \mu = 0{\cdot}25, \; t_0 = 0, \; t_1 = 6,$$

$$\Delta x = \Delta y = a/12, \; \Delta z = d/12.$$

A constant, uniformly distributed load $q = 0{\cdot}6\,\text{kp cm}^{-2}$, applied in time t_0, was considered. The results furnished by computer analysis (IBM 7094) are given in Table 2 for various numbers, n, of subintervals in time, and are graphically represented in Figs. 5a, b, c). Figure 6 gives an example how the plots were output on printer. For practical purposes the line plots in Fig. 5 need not be constructed because the letter code in the printer plot as in Fig. 6 enables to determine the value in any point (without interpolation) with the accuracy of ± 1 per cent of the maximum value.

Finally, the comparison of computer storage requirements is of interest. Denoting by N the number of storage locations required for the first order method for rate-type creep,

TABLE 2. NUMERICAL RESULTS FOR RATE-TYPE CREEP OF A PLATE

Method	Subdivision n	$x = a/2$ $y = b/2$ w	$x = a/3$ $y = b/2$ w	$x = a/2$ $y = b/2$ $z = d/2$ σ_x	$x = a/2$ $y = b/2$ $z = d/2$ σ_y	$x = b/3$ $y = b/6$ $z = d/2$ τ_{xy}	$x = a/2$ $y = b/2$ $z = d/3$ σ_x
1st order	4	1·06396	0·86732	132·11	118·22	−11·426	103·96
method	8	1·06130	0·86480	131·96	117·55	−11·717	103·19
	16	1·06082	0·86440	131·92	117·19	−11·847	102·87
	32	1·06054	0·86430	131·90	117·01	−11·908	102·72
	64	1·06052	0·86427	131·89	116·92	−11·938	102·65
2nd order	4	1·05716	0·86075	131·69	115·65	−11·971	102·28
method	8	1·06030	0·86378	131·89	116·72	−11·979	102·53
	16	1·06070	0·86415	131·88	116·81	−11·9701	102·565
	32	1·06079	0·86423	131·883	116·825	−11·9679	102·573
	64	1·06081	0·86424	131·884	116·829	−11·9674	102·575

the second order method for rate-type creep requires about $2N$ locations. The fourth order method for integral-type creep requires $(n+4)N$ locations where n is the number of subdivisions of the time interval. In the case of a degenerate memory function, however, the number of storage locations needed is the same as for the rate-type creep (for a method of the same order), and the computer time is also about the same.

5. CONCLUSIONS

1. The non-linear creep of plates, either of integral-type or of rate-type, can be solved as a sequence of elasticity problems.

2. In the problem considered, the algorithms in Figs. 1 and 4 practically well converged and enabled to achieve highly accurate results.

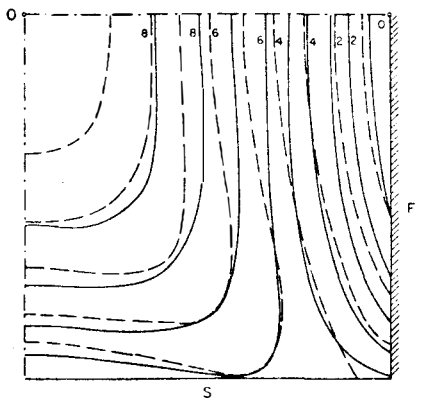

FIG. 5(a).

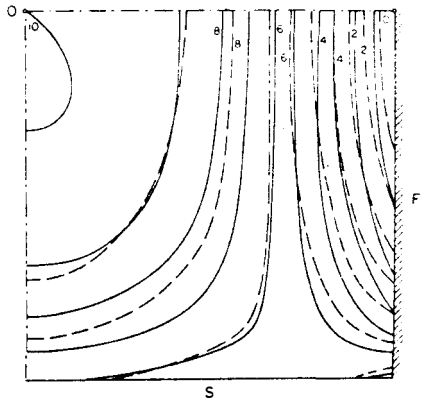

FIG. 5(b).

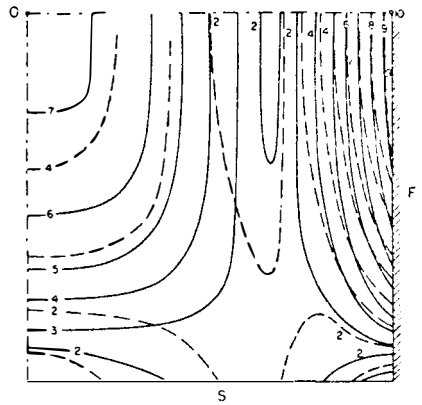

FIG. 5(c).

FIG. 5. Lines of equal relative values in the right lower quadrant of plate. Rate-type creep. (Dashed lines pertain to $t = t_0$, continuous lines to $t = t_1$; S denotes the simply supported edge, F the fixed edge, 0 the center of plate.) (a) Maximum principal stresses at the lower face of plate; in time t_0, 0 corresponds to −67, 10 to 129·8;
lower face; in time t_0, 0 corresponds to −267, 10 to 94·5; in time t_1, 0 corresponds to −200, 10 to 116·8.
(c) Stress intensity at the faces; in time t_0, 0 corresponds to 0, 10 to 244; in time t_1, 0 corresponds to 0, 10 to 175.

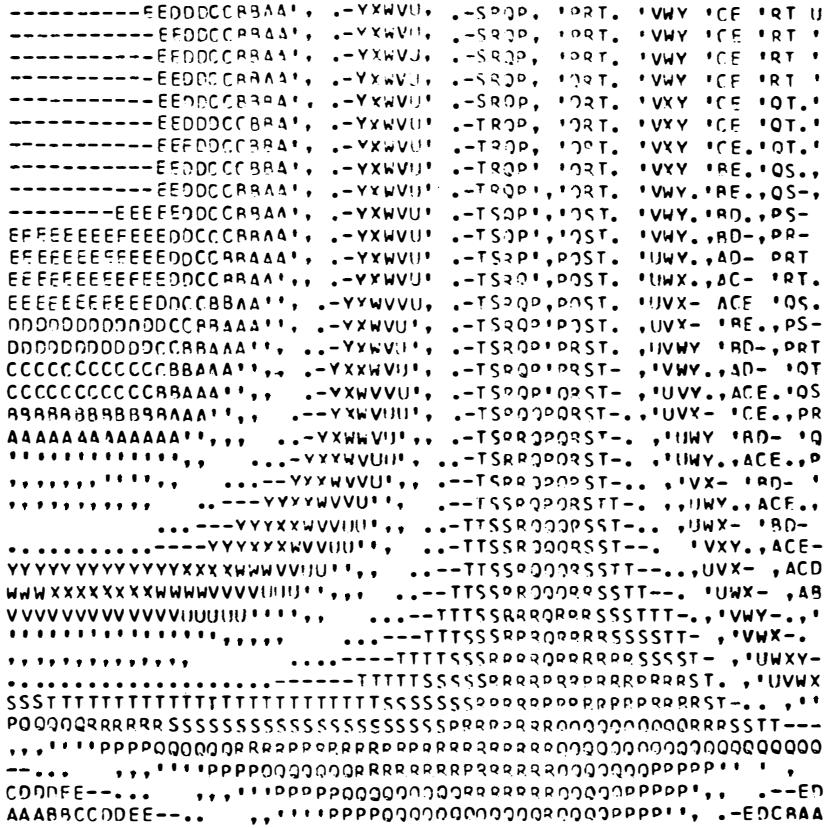

FIG. 6. Example showing how the lines of equal values [in Fig. 5(c), $t = t_1$] were simulated on printer. (The interval between the maximum value and the minimum value was divided in 50 equal subintervals, to which the following series of 50 characters was assigned.

ABCDE-. .'PQRST-. .'UVWXY-. .'ABCDE-. .'PQRST-. .').

3. For the integral-type creep (flow chart in Fig. 1), high number of iterations per step brings hardly any improvement of accuracy and two iterations per step ($n_j = 2$) are sufficient.

4. In the case of rate-type creep, the convergence rate of the second-order method was for stresses in some nodes substantially better than in the first order method, while in other nodes the convergence rate was about the same (but not worse).

5. For a degenerate memory function [equation (9)] the requirements for storage and computer time may be substantially reduced and become comparable with the requirements in the case of rate-type creep.

6. The finite difference method in space coordinates is suitable for the plates with simple boundaries, such as the rectangular plates.

Acknowledgement The present research was sponsored by Ford Science Foundation and carried out during 1967 68 at the University of Toronto, Department of Civil Engineering, under the supervision of Professor M. W. Huggins

REFERENCES

[1] T. H. LIN, *Theory of inelastic structures* J. Wiley (1968).
[2] Z. P. BAŽANT, Linear creep solved by a succession of generalized thermo-elasticity problems. *Acta tech (Praha)* 5, 581–594 (1967). [See also Time redistributions of stress and strain at non-homogeneous creep (in Czech). Report No. 75.66, Building Research Institute, ČVUT, Prague (1966).]
[3] Z. P. BAŽANT, Approximate methods of analysis of creep and shrinkage of nonhomogeneous structures and use of computers (in Czech). *Stav. Čas.* 7, 414–431 (1964).
[4] Z. P. BAŽANT, Concrete Creep in Structural Analysis, (in Czech). SNTL (1966).
[5] T. H. LIN and J. K. GANOUNG, Bending of rectangular plates with nonlinear creep. *Int. J. mech. Sci.* 6, 337–348 (1964).
[6] O. C. ZIENKIEWICZ and Y. K. CHEUNG, *The Finite Element Method in Structural and Continuum Mechanics*. McGraw Hill (1967).
[7] S. P. TIMOSHENKO and S. WOINOWSKY-KRIEGER, *Theory of Plates and Shells*, 2nd edition. McGraw-Hill (1959).
[8] K. REKTORYS *et al.*, *Survey of Applicable Mathematics*. Iliffe Books (1969).
[9] Z. P. BAŽANT, Creep analysis of one- or two-dimensional structures, (in Czech), Report No. 80.66, Building Research Institute, ČVUT, Prague (1966).

APPENDIX

Theorem 1

Let the constitutive equation for small strains be

$$\sigma_{ij} = c_{ijkl}(\varepsilon_{kl} - \varepsilon^0_{kl}) \tag{A1}$$

where σ_{ij} = stress tensor, ε_{kl} = strain tensor, ε^0_{ij} = initial strain tensor, c_{ijkl} = elastic moduli; c_{ijkl} and ε^0_{ij} may depend on space coordinates $x_i (i = 1, 2, 3)$. Introduce the prestress tensor

$$\sigma^0_{ij} = c_{ijkl}\varepsilon^0_{kl} \tag{A2}$$

and define $\mathbf{F}^1$ as the state of volume and surface loads which equilibrate σ^0_{ij}. Then, in a given body under zero applied load, the stresses are $\sigma^1_{ij} - \sigma^0_{ij}$, the (linearized) strains are ε^1_{ij} and the (small) displacements are u^1_i where $\sigma^1_{ij}, \varepsilon^1_{ij}, u^1_i$ is the solution of the same body (with the given prescribed displacements) for loads $\mathbf{F}^1$ and zero initial strains ($\varepsilon^0_{ij} = 0$).

Effect of initial strains in plates

Consider a plate in plane (x, y) or (x_1, x_2). To determine the effect of initial strains $\varepsilon^0_{w(r)}, \varepsilon^0_{11(r)}, \varepsilon^0_{22(r)}, \varepsilon^0_{12(r)}, \varepsilon^0_{33(r)}$ given by equation (5), first the prestresses defined by equation (6) must be computed, as required by Theorem 1. For substitution in formula (6), it is

necessary to calculate first the deviatoric and volumetric components which are ($\sigma_{33_{(s)}} = \sigma_{13_{(s)}} = \sigma_{23_{(s)}} = 0$):

$$s_{11_{(s)}} = \sigma_{11_{(s)}} - \sigma_{v_{(s)}},\ s_{22_{(s)}} = \sigma_{22_{(s)}} - \sigma_{v_{(s)}},\ s_{12_{(s)}} = \sigma_{12_{(s)}};\qquad \sigma_{v_{(s)}} = (\sigma_{11_{(s)}} + \sigma_{22_{(s)}})/3 \quad \text{(A3)}$$

The resultants of prestresses (6) over the thickness of the plate are certain bending moments, denoted as $M^0_{x_{(r)}}$ and $M^0_{y_{(r)}}$, and torsional moment $M^0_{xy_{(r)}}$.

$$M^0_{x_{(r)}} = \int_{-d/2}^{+d/2} \sigma^0_{11_{(r)}} z\,\mathrm{d}z, \qquad M^0_{y_{(r)}} = \int_{-d/2}^{+d/2} \sigma^0_{22_{(r)}} z\,\mathrm{d}z, \qquad M^0_{xy_{(r)}} = \int_{-d/2}^{+d/2} \sigma^0_{12_{(r)}} z\,\mathrm{d}z \quad \text{(A4)}$$

where

$$\sigma^0_{11_{(r)}} = \sigma^0_{v_{(r)}} + s^0_{11_{(r)}}, \qquad \sigma^0_{22_{(r)}} = \sigma^0_{v_{(r)}} + s^0_{22_{(r)}}, \qquad \sigma^0_{12_{(r)}} = s^0_{12_{(r)}}. \quad \text{(A5)}$$

According to the well-known differential equilibrium equation for plates [7] the distributed load $q^1_{(r)}$ which balances $\sigma^0_{v_{(r)}}, s^0_{11_{(r)}}, s^0_{22_{(r)}}, s^0_{12_{(r)}}$ is

$$q^1_{(r)} = -\frac{\partial^2 M^0_{x_{(r)}}}{\partial x^2} - 2\frac{\partial^2 M^0_{xy_{(r)}}}{\partial x \partial y} - \frac{\partial^2 M^0_{y_{(r)}}}{\partial y^2}. \quad \text{(A6)}$$

This load represents the loading state $\mathbf{F}^1$, defined in Theorem 1. In addition, $\mathbf{F}^1$ might also include certain loads at the edges. But at simply supported edges $\sigma^0_{ij_{(r)}}$ and $M^0_{x_{(r)}}, \ldots$ are all zero so that no loads are needed. At fixed edges, moments balancing $M^0_{x_{(r)}}, \ldots$ should be included in $\mathbf{F}^1$; they have, however, no effect on the stresses in the plate.

Deflection $w^1_{(r)}$ of the elastic plate under the load $q^1_{(r)}$ may be solved from the equation [7]:

$$\left(\frac{\partial^2}{\partial x^2} + \frac{\partial^2}{\partial y^2}\right)^2 w^1_{(r)} = \frac{q^1_{(r)}}{D} \quad \text{(A7)}$$

with the appropriate boundary conditions; notation: $D = \frac{1}{12}d^3E/(1-\mu^2)$ where $E = 3/(K^{-1} + G^{-1})$ = Young modulus, $\mu = (\frac{1}{2}K - G)/(K+G)$ = Poisson ratio. The stresses $\sigma^1_{ij_{(r)}}$ due to $q^1_{(r)}$ are determined from the relationships [7]:

$$\left.\begin{aligned} \sigma^1_{11_{(r)}} &= -\frac{Ez}{1-\mu^2}\left(\frac{\partial^2 w_{(r)}}{\partial x^2} + \mu\frac{\partial^2 w_{(r)}}{\partial y^2}\right), \qquad \sigma^1_{22} = -\frac{Ez}{1-\mu^2}\left(\frac{\partial^2 w_{(r)}}{\partial y^2} + \mu\frac{\partial^2 w_{(r)}}{\partial x^2}\right) \\ \sigma^1_{12_{(r)}} &= -Gz\frac{\partial^2 w_{(r)}}{\partial x \partial y} \end{aligned}\right\}. \quad \text{(A8)}$$

Finally, the deflections and stresses, caused by the initials strains $\varepsilon^0_{v_{(r)}}, e^0_{11_{(r)}}, e^0_{22_{(r)}}, e^0_{12_{(r)}}, e^0_{33_{(r)}}$, are:

$$w_{(r)} = w^1_{(r)}, \quad \sigma_{11_{(r)}} = \sigma^1_{11_{(r)}} - \sigma^0_{11_{(r)}}, \qquad \sigma_{22_{(r)}} = \sigma^1_{22_{(r)}} - \sigma^0_{22_{(r)}}, \qquad \sigma_{12_{(r)}} = \sigma^1_{12_{(r)}} - \sigma^0_{12_{(r)}}. \quad \text{(A9)}$$

Relationships (A4)–(A9) were derived in 1964 independently by Lin [5] and by Bažant [3]. More general relationships for sandwich plates and shells have been also deduced [9].

(*Received* 17 *February* 1969; *revised* 20 *January* 1970)

Абстракт—Дается общий численный метод интегрированиа по времени нелинейных задач ползучести наследственного типа. Предлагаемый метод сводит задачу ползучести к ряду задач упругости с вынужденными деформациями. Проверяется практическая вероятность и сходимость на основе расчета прямоугольной пластинки. Исследуется эмпирически точность разного рода методов. Для специального случая вырожденного ядра последействия выводится эффективная, по экономии машинного вычисления, модификация метода. Кроме того исследуются численные методы для дифференуиального зачона ползучести.